



Standard Test Method for Determination of Slow Crack Growth Parameters of Advanced Ceramics by Constant Stress Flexural Testing (Stress Rupture) at Elevated Temperatures¹

This standard is issued under the fixed designation C1834; the number immediately following the designation indicates the year of original adoption or, in the case of revision, the year of last revision. A number in parentheses indicates the year of last reapproval. A superscript epsilon (ε) indicates an editorial change since the last revision or reapproval.

1. Scope

1.1 This test method covers the determination of the slow crack growth (SCG) parameters of advanced ceramics in a given test environment at elevated temperatures in which the time-to-failure of four-point- $\frac{1}{4}$ point flexural test specimens (see Fig. 1) is determined as a function of different levels of constant applied stress. This SCG constant stress test procedure is also called a slow crack growth (SCG) stress rupture test. The test method addresses the test equipment, test specimen fabrication, test stress levels and experimental procedures, data collection and analysis, and reporting requirements.

1.2 In this test method the decrease in time-to-failure with increasing levels of applied stress in specified test conditions and temperatures is measured and used to analyze the slow crack growth parameters of the ceramic. The preferred analysis method is based on a power law relationship between crack velocity and applied stress intensity; alternative analysis approaches are also discussed for situations where the power law relationship is not applicable.

NOTE 1—This test method is historically referred to in earlier technical literature as static fatigue testing (Refs 1-3)² in which the term fatigue is used interchangeably with the term *slow crack growth*. To avoid possible confusion with the fatigue phenomenon of a material that occurs exclusively under cyclic stress loading, as defined in E1823, this test method uses the term *constant stress testing* rather than static fatigue testing.

1.3 This test method uses a 4-point- $\frac{1}{4}$ point flexural test mode and applies primarily to monolithic advanced ceramics that are macroscopically homogeneous and isotropic. This test method may also be applied to certain whisker- or particle-reinforced ceramics as well as certain discontinuous fiber-reinforced composite ceramics that exhibit macroscopically homogeneous behavior. Generally, continuous fiber ceramic composites do not exhibit macroscopically isotropic,

homogeneous, elastic continuous behavior, and the application of this test method to these materials is not recommended.

1.4 This test method is intended for use at elevated temperatures with various test environments such as air, vacuum, inert gas, and steam. This test method is similar to Test Method C1576 with the addition of provisions for testing at elevated temperatures to establish the effects of those temperatures on slow crack growth. The elevated temperature testing provisions are derived from Test Methods C1211 and C1465.

1.5 Creep deformation at elevated temperatures can occur in some ceramics as a competitive mechanism with slow crack growth. Those creep effects may interact and interfere with the slow crack growth effects (see 5.5). This test method is intended to be used primarily for ceramic test specimens with negligible creep. This test method imposes specific upper-bound limits on measured maximum creep strain at fracture or run-out (no more than 0.1 %, in accordance with 5.5).

1.6 The values stated in SI units are to be regarded as the standard and in accordance with IEEE/ASTM SI 10.

1.7 *This standard does not purport to address all of the safety concerns, if any, associated with its use. It is the responsibility of the user of this standard to establish appropriate safety and health practices and determine the applicability of regulatory limitations prior to use.*

2. Referenced Documents

2.1 ASTM Standards:³

- C1145 Terminology of Advanced Ceramics
- C1161 Test Method for Flexural Strength of Advanced Ceramics at Ambient Temperature
- C1211 Test Method for Flexural Strength of Advanced Ceramics at Elevated Temperatures
- C1239 Practice for Reporting Uniaxial Strength Data and Estimating Weibull Distribution Parameters for Advanced Ceramics

¹ This test method is under the jurisdiction of ASTM Committee C28 on Advanced Ceramics and is the direct responsibility of Subcommittee C28.01 on Mechanical Properties and Performance.

Current edition approved Feb. 1, 2016. Published April 2016. DOI: 10.1520/C1834-16.

² The boldface numbers in parentheses refer to the list of references at the end of this standard.

³ For referenced ASTM standards, visit the ASTM website, www.astm.org, or contact ASTM Customer Service at service@astm.org. For *Annual Book of ASTM Standards* volume information, refer to the standard's Document Summary page on the ASTM website.

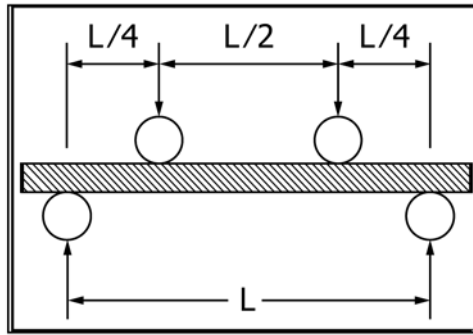


FIG. 1 Four-point- $\frac{1}{4}$ Point Flexural Test Schematic

C1291 Test Method for Elevated Temperature Tensile Creep Strain, Creep Strain Rate, and Creep Time-to-Failure for Advanced Monolithic Ceramics

C1322 Practice for Fractography and Characterization of Fracture Origins in Advanced Ceramics

C1368 Test Method for Determination of Slow Crack Growth Parameters of Advanced Ceramics by Constant Stress-Rate Strength Testing at Ambient Temperature

C1465 Test Method for Determination of Slow Crack Growth Parameters of Advanced Ceramics by Constant Stress-Rate Flexural Testing at Elevated Temperatures

C1576 Test Method for Determination of Slow Crack Growth Parameters of Advanced Ceramics by Constant Stress Flexural Testing (Stress Rupture) at Ambient Temperature

E4 Practices for Force Verification of Testing Machines

E112 Test Methods for Determining Average Grain Size

E220 Test Method for Calibration of Thermocouples By Comparison Techniques

E230 Specification and Temperature-Electromotive Force (EMF) Tables for Standardized Thermocouples

E337 Test Method for Measuring Humidity with a Psychrometer (the Measurement of Wet- and Dry-Bulb Temperatures)

E399 Test Method for Linear-Elastic Plane-Strain Fracture Toughness K_{Ic} of Metallic Materials

E1823 Terminology Relating to Fatigue and Fracture Testing

IEEE/ASTM SI 10 American National Standard for Use of the International System of Units (SI): The Modern Metric System

3. Terminology

3.1 Definitions:

3.1.1 The terms described in Terminology C1145 and Terminology E1823 are applicable to this test method. Specific terms relevant to this test method are as follows:

3.1.2 *advanced ceramic, n*—a highly engineered, high performance, predominately non-metallic, inorganic, ceramic material having specific functional attributes. C1145

3.1.3 *constant applied stress, $\sigma[FL^{-2}]$, n*—a constant maximum flexural stress applied to a specified beam test specimen by using a constant static force with a test machine and a test fixture. C1576

3.1.4 *constant applied stress versus time-to-failure diagram, n*—a plot of constant applied stress against time-to-failure for experimental test data. (See Fig. 2)

3.1.4.1 *Discussion*—Constant applied stress and time-to-failure are both plotted on logarithmic scales. Data may be organized and plotted by experimental test temperature. Also called an SCG stress rupture diagram. (See Fig. 2) C1576

3.1.5 *constant applied stress versus time-to-failure curve, n*—a curve fitted to the values of time-to-failure at each of several applied stresses. (See Fig. 2)

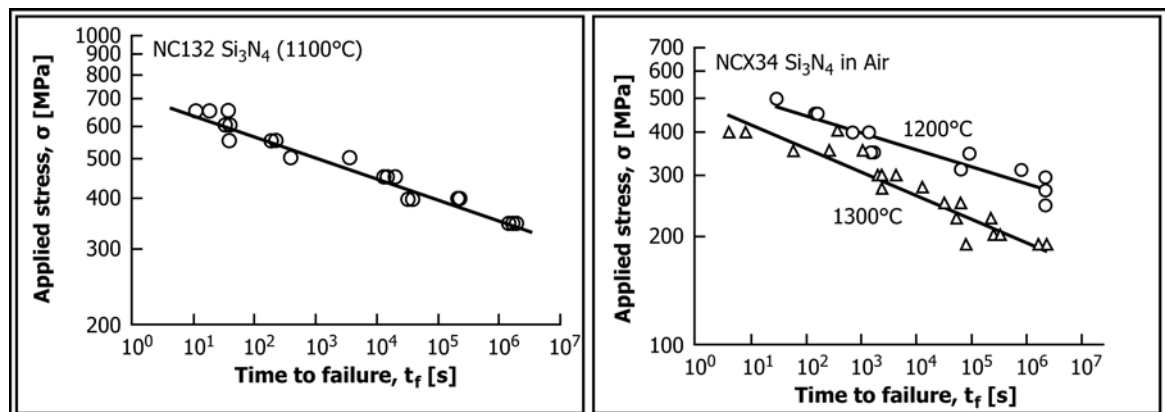


FIG. 2 Examples of Applied Stress versus Time-to-Failure Diagrams [NC132 Silicon Nitride at 1100°C in Air (Ref 28) and NCX34 Silicon Nitride at 1200°C and 1300°C in Air (Ref 29)]

3.1.5.1 *Discussion*—In the historical ceramics literature, the constant applied stress versus time-to-failure curve is often called a static fatigue curve. A more accurate descriptive name is a slow crack growth (SCG) stress rupture curve. **C1576**

3.1.6 *crack-extension resistance*, $K_R [FL^{-3/2}]$, $G_R [FL^{-1}]$ or $J_R [FL^{-1}]$, n —a measure of the resistance of a material to crack extension expressed in terms of the stress-intensity factor, K ; crack-extension force, G ; or values of J derived using the J -integral concept. **E1823**

3.1.6.1 *Discussion*—The J -integral concept in this **E1823** definition is a metal fracture concept and is not applicable to brittle ceramics.

3.1.7 *creep strain*, n —the time-dependent strain that occurs after the application of a force which is thereafter maintained constant. **C1291**

3.1.8 *dead weight test machine*, n —a mechanical testing machine which uses a load frame, lever-arms, and an adjustable weight train (with calibrated dead weights) to apply a constant known force to the test specimen over an extended period of time.

3.1.9 *flexural strength*, $\sigma_f [FL^{-2}]$, n —a measure of the ultimate strength of a specified beam test specimen in flexure determined at a given stress in a particular environment. **C1576**

3.1.10 *fracture toughness*, n —a generic term for measures of resistance to extension of a crack. **E399, E1823**

3.1.11 *inert flexural strength* $[FL^{-2}]$, n —the flexural strength of a specified beam as determined in an inert test condition whereby no slow crack growth occurs.

3.1.11.1 *Discussion*—An inert condition may be obtained by testing at a low temperature, at a very fast test rate, or in an inert test environment such as vacuum, silicone oil, high purity dry N_2 , or liquid nitrogen. **C1465**

3.1.12 *plane-strain fracture toughness*, (*critical stress intensity factor*) $K_{IC} [FL^{-3/2}]$, n —the crack extension resistance under conditions of crack-tip plane strain in Mode I for slow rates of loading under predominantly linear-elastic conditions and negligible plastic-zone adjustment. **E1823**

3.1.13 *R-curve*, n —a plot of crack-extension resistance as a function of stable crack extension. **C1145**

Also defined as a K-R curve. **E1823**

3.1.14 *run-out*, n —a test specimen that does not fail before a prescribed test time limit. **C1576**

3.1.15 *slow crack growth (SCG)*, n —subcritical crack growth (extension) which may result from, but is not restricted to, such mechanisms as environmentally-assisted stress corrosion or diffusive crack growth. **C1368, C1465, C1576**

3.1.16 *slow crack growth (SCG) parameters*, n —the parameters estimated as constants in the log (*time-to-failure*) versus log (*constant applied stress*), which represent a measure of the susceptibility to slow crack growth of a material (see **Appendix X1**). **C1465**

3.1.17 *stress intensity factor*, $K_I [FL^{-3/2}]$, n —the magnitude of the ideal-crack-tip stress field stress field singularity) subjected to Mode I loading in a homogeneous, linear elastic body. **E1823**

3.1.18 *test environment*, n —the aggregate of chemical species and energy that surrounds a test specimen. **E1823**

3.1.19 *test environmental chamber*, n —a container surrounding the test specimen that is capable of providing a controlled local environmental condition. **C1368, C1465**

3.1.20 *time-to-failure*, $t_f [t]$, n —total elapsed time from test initiation to test specimen failure/rupture for a defined test condition.

4. Significance and Use

4.1 The service life of many structural ceramic components is often limited by the subcritical growth of cracks over time, under stress at a defined temperature, and in a defined chemical environment (Refs **1-3**). When one or more cracks grow to a critical size, brittle catastrophic failure may occur in the component. Slow crack growth in ceramics is commonly accelerated at elevated temperatures. This test method provides a procedure for measuring the long term load-carrying ability and appraising the relative slow crack growth susceptibility of ceramic materials at elevated temperatures as a function of time, temperature, and environment. This test method is based on Test Method **C1576** with the addition of provisions for elevated temperature testing.

4.2 This test method is also used to determine the influences of processing variables and composition on slow crack growth at elevated temperatures, as well as on strength behavior of newly developed or existing materials, thus allowing tailoring and optimizing material processing for further modification.

4.3 This test method may be used for material development, quality control, characterization, design code or model verification, time-to-failure, and limited design data generation purposes.

NOTE 2—Data generated by this test method do not necessarily correspond to crack velocities that may be encountered in service conditions. The use of data generated by this test method for design purposes, depending on the range and magnitude of applied stresses used, may entail extrapolation and uncertainty.

4.4 This test method and Test Method **C1576** are similar and related to Test Methods **C1368** and **C1465**; however, **C1368** and **C1465** use constant stress-rates (linearly increasing stress over time) to determine corresponding flexural strengths, whereas this test method and **C1576** employ a constant stress (fixed stress levels over time) to determine corresponding times-to-failure. In general, the data generated by this test method may be more representative of actual service conditions as compared with data from constant stress-rate testing. However, in terms of test time, constant stress testing is inherently and significantly more time consuming than constant stress-rate testing.

4.5 The flexural stress computation in this test method is based on simple elastic beam theory, with the following assumptions: the material is isotropic and homogeneous; the moduli of elasticity in tension and compression are identical; and the material is linearly elastic. These assumptions are based on small grain size in the ceramic specimens. The grain size should be no greater than $1/50$ of the beam depth as measured by the mean linear intercept method (**E112**). In cases

where the material grain size is bimodal or the grain size distribution is wide, the limit should apply to the larger grains.

4.6 The test specimen sizes and test fixtures have been selected in accordance with Test Method C1211 which provides a balance between practical configurations and resulting errors, as discussed in Refs 4 and 5. Test Method C1211 also specifies fixture material requirements for elevated test temperature stability and functionality.

4.7 The SCG data are evaluated by regression of log applied-stress vs. log time-to-failure to the experimental data. The recommendation is to determine the slow crack growth parameters by applying the power law crack velocity function. For derivation of this, and for alternative crack velocity functions, see Appendix X1.

NOTE 3—A variety of crack velocity functions exist in the literature. A comparison of the functions for the prediction of long-term constant stress (static fatigue) data from short-term constant stress rate (dynamic fatigue) data (Ref 6) indicates that the exponential forms better predict the data than the power-law form. Further, the exponential form has a theoretical basis (Refs 7-10); however, the power law form is simpler mathematically. Both forms have been shown to fit short-term test data well.

4.8 The approach used in this test method assumes that the ceramic material displays no rising R-curve behavior, that is, no increasing fracture resistance (or crack-extension resistance) with increasing crack length for a given test temperature. The existence of such R-curve behavior cannot be determined from this test method. The analysis further assumes that the same flaw type controls all times-to-failure for a given test temperature.

4.9 Slow crack growth behavior of ceramic materials can vary as a function of material properties, thermal conditions, and environmental variables. Therefore, it is essential that test results accurately reflect the effects of the specific variables under study. Only then can data be compared from one investigation to another on a valid basis, or serve as a valid basis for characterizing materials and assessing structural behavior.

4.10 Like mechanical strength, the SCG time-to-failure of advanced ceramics is probabilistic in nature. Therefore, slow crack growth that is determined from times-to-failure under given constant applied stresses is also a probabilistic phenomenon. The scatter in time-to-failure in constant stress testing is much greater than the scatter in strength in constant stress-rate (or any strength) testing (Refs 1, 11-13; see Appendix X2). Hence, a proper range and number of constant applied stress levels, in conjunction with an appropriate number of test specimens, are required for statistical reproducibility and reliable design data generation (Ref 1-3). This test method provides guidance in this regard.

4.11 The time-to-failure of a ceramic material for a given test specimen and test fixture configuration is dependent on the ceramic material's inherent resistance to fracture, the presence of flaws, the applied stress, and the temperature and environmental effects. Fractographic analysis to verify the failure mechanisms has proven to be a valuable tool in the analysis of SCG data to verify that the same flaw type is dominant over the entire test range (Refs 14, 15), and fractography is recommended in this test method (refer to Practice C1322).

5. Interferences

5.1 Slow crack growth (SCG) may be the product of both mechanical stress and chemical driving forces. The chemical driving force for a given material may vary strongly with the chemistry and temperature of the test environment. SCG testing is conducted at temperatures and in environments representative of service conditions, so as to evaluate material performance under service conditions. Note that slow crack growth testing, particularly constant stress testing, is very time consuming. The overall test time is considerably greater in constant stress testing than in constant stress-rate testing. Because of this longer test time, the temperature and chemical variables of the test environment shall be controlled to minimize changes during the test. Inadequate control of temperature and environmental conditions may result in inaccurate time-to-failure data, especially for materials that are more sensitive to elevated temperatures and reactive environments.

5.2 A wide range of different interference effects can occur in slow crack growth testing at elevated temperatures (Refs 16-27).

5.2.1 Creep damage (cavitation and micro-cracks) on or near the tensile surface of the test specimen.

5.2.2 Creep-induced non-linear stress-strain effects on the tensile surface of the test specimen.

5.2.3 Differences in creep strain on the tensile surface versus the compressive surface of the test specimen introducing non-linear stress-strain effects through the thickness of the test specimen.

5.2.4 Deviations in the linear relationship between log (constant applied stress) and log (time-to-failure) at high stress levels.

5.2.5 Oxidation induced crack healing and crack tip blunting.

5.2.6 Chemical reactions, oxidation, phase changes, and devitrification of grain boundary layers in the ceramics.

5.3 Variations in the test specimens and the experimental conditions can also act as interferences.

5.3.1 Different flaw populations between the surface and the interior of the test specimen.

5.3.2 Surface condition effects and anomalous surface flaws from specimen machining and grinding.

5.3.3 Non-uniform test specimen dimensions (dimensional variations, warp, twist, and bowing).

5.3.4 Localized fracture from contact and friction stresses at load points.

NOTE 4—These issues are discussed in detail in Annex A1 and in Test Methods C1211 and C1291.

5.4 All of these effects may change the stress conditions, the flaw populations, and the crack growth mechanisms in the test specimens. These factors need to be considered, accounted for, and controlled for each given test material and set of test conditions.

5.5 Creep deformation and effects may be a primary interference in high temperature SCG testing. Significant creep at both higher temperatures and longer test times may produce nonlinearity in stress-strain relations as well as accumulated tensile damage in flexure (Ref 11). This, depending on the

degree of nonlinearity, may limit the applicability of linear elastic fracture mechanics (LEFM), since the resulting relationship between strength and stress derived under constant stress testing condition is based on an LEFM approach with negligible creep (maximum creep strain less than 0.1 %). Therefore creep strain should be minimized as much as possible (to no more than 0.1 %), as compared to the total elastic strain at failure (see Fig. 3 and 8.9.2).

6. Apparatus

6.1 *Test Machine*—Dead weight test machines or universal test machines capable of maintaining a constant applied force shall be used for constant stress testing. Test machines used for this test method shall conform to the requirements of Practice E4. The applied force shall be monitored during the test and the variations in the applied force shall not exceed ± 1.0 % of the nominal value at any given time during the test.

6.1.1 Universal test machines shall meet the system compliance requirements as cited in Annex A2 and Test Method C1211, section 6.9. Dead-weight machines do not have any compliance requirements.

6.2 *Test Fixtures*—The configurations and mechanical properties of test fixtures shall be in accordance with Test Method C1211. The materials from which the test fixtures, including bearing cylinders, are fabricated shall be effectively inert to the test environment at the test temperatures, so that they do not significantly react with or contaminate either the test specimen or the test environment. In addition, the test fixtures shall remain elastic under test temperatures and loading conditions.

NOTE 5—Various grades of silicon carbide (such as hot-pressed or sintered) and high-purity aluminas are candidate materials for test fixtures as well as load train components in the hot zone. The load-train material should also be effectively inert to the test environment. For more specific information regarding use of appropriate materials for fixtures and load train with respect to test temperatures, refer to Section 6 of Test Method C1211.

6.2.1 *Four-Point Flexure*—The four-point- $\frac{1}{4}$ point fixture described in Test Method C1211, Section 6.2, shall be used in this test method (see Fig. 1). The nominal outer (support) spans (L) for the A, B, and C test fixtures are $L = 20$ mm, 40 mm, and 80 mm, respectively. Three-point flexure shall not be used.

6.2.2 *Bearing Cylinders*—The requirements of dimensions and mechanical properties of bearing cylinders as described in Test Method C1211 shall be used in this test method. The

bearing cylinders shall be free to roll in order to relieve frictional constraints, as described in Test Method C1211.

6.2.3 *Semiarticulating Four-Point Fixture*—The semiarticulating four-point fixture is described in Test Method C1211. Use the semiarticulating test fixture for test specimens that meet the parallelism requirements of Test Method C1211.

6.2.4 *Fully Articulating Four-Point Fixture*—The fully articulating four-point fixture is described in Test Method C1211. Use the fully articulating test fixture for test specimens that do not meet the parallelism requirements in Test Method C1211, due to the ceramic fabrication process (as-fired, heat-treated or oxidized).

6.3 *Heating Apparatus*—The heating system (such as furnace enclosure, heating elements, thermal control, temperature measuring device, or thermocouple, or combinations thereof) shall conform to the requirements in Test Method C1211, section 6.11.

6.3.1 *Test Furnace and Temperature Readout Device*—The furnace shall be capable of maintaining the test specimen temperature within $\pm 2^\circ\text{C}$ during each testing period. The temperature readout device shall have a resolution of 1°C or smaller. The furnace system shall be such that thermal gradients are minimal along the length of the test specimen with no more than a 5°C differential from end-to-end in the test specimen.

NOTE 6—Tests are sometimes conducted in furnaces that have thermal gradients. Test specimens of smaller sizes will reduce thermal gradient problems, but it is essential to monitor the temperature along the length of the test specimen.

6.3.2 Thermocouples:

6.3.2.1 The specimen temperature shall be monitored by a thermocouple with its tip situated no more than 1 mm from the midpoint of the test specimen. Either a fully sheathed or exposed bead junction may be used. If a sheathed tip is used, verify that there is negligible error associated with the covering sheath.

(1) Thermocouple integrity and stability are significant concerns at elevated temperatures and long exposure times. Exposed thermocouple beads have greater sensitivity, but they may be exposed to vapors that may react with the thermocouple materials. (For example, silica vapors will react with platinum.) Beware of the use of heavy-gage thermocouple wire, thermal gradients along the thermocouple length, or

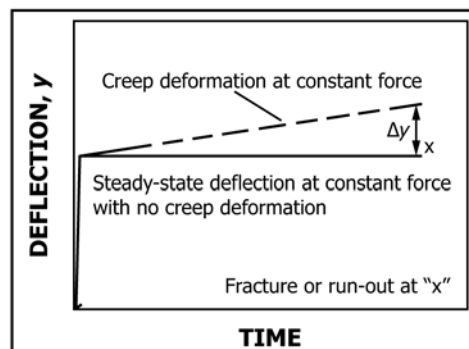


FIG. 3 Creep Deformation and Deflection at Constant Force Conditions

excessively heavy-walled insulators, all of which may lead to erroneous temperature readings.

(2) The thermocouple tip may contact the test specimen, but only if there is certainty that the thermocouple tip or sheathing material will not interact chemically with the test specimen. Thermocouples may be prone to breakage if they are in contact with the test specimen.

6.3.2.2 A separate thermocouple may be used to control the furnace, if necessary, but the test specimen temperature shall be the reported temperature of the test.

6.3.2.3 The thermocouple(s) shall be calibrated in accordance with Test Method E220 and Specification and Tables E230. The thermocouples shall be periodically checked since calibration may drift with usage or contamination.

6.3.2.4 The measurement of temperature shall be accurate to within $\pm 5^{\circ}\text{C}$. The accuracy shall include the error inherent to the thermocouple as well as any errors in the measuring instruments.

NOTE 7—Resolution should not be confused with accuracy. Beware of recording instruments that read out to 1°C (resolution) but have an accuracy of only $\pm 10^{\circ}\text{C}$ or $\pm \frac{1}{2}\%$ of full-scale (for example, $\frac{1}{2}\%$ of 1200°C is 6°C).

NOTE 8—Temperature measuring instruments typically approximate the temperature-electromotive force (EMF, in millivolt) tables, and may have an error of a few degrees.

6.3.2.5 The appropriate thermocouple extension wire shall be used to connect a thermocouple to the furnace controller and temperature readout device, which shall have either a cold junction or a room-temperature compensation circuit. Special care should be directed toward connecting the extension wire with the correct polarity.

6.4 *Furnace Environmental Chamber*—The furnace may have an air, inert, vacuum, or any other gaseous environment, as required. If testing is conducted in any gaseous environment other than ambient air, an appropriate environmental chamber shall be constructed to facilitate handling, control, and monitoring of the test environment so that constant test environment conditions can be maintained. The chamber shall be effectively corrosion-resistant to the test environment so that it does not react with or change the environment. If the load train acts through bellows, fittings, or seals, verify that force losses or errors do not exceed 1% of the prospective failure forces.

6.5 *Deflection Measurement*—Beam deflection and outer fiber strain (strain at the outer face of the flexure beam) measurements are not needed to calculate a slow crack growth parameter. However, deflection measurements may be necessary for determining if significant creep deformation is occurring. Deflection measurement of test specimens for creep is particularly important for certain ceramic materials at higher test temperatures and longer test times and is highly recommended to ensure that maximum creep strain of those ceramic specimens is within the allowable limit (see 8.9.2).

6.5.1 Creep deformation can be measured by three methods: real-time in-situ deflection of the midpoint or load points of the test specimen, crosshead displacement, and post-test measurement of the permanent deformation of the midpoint of the test specimen.

6.5.2 Deflection-measuring equipment shall be capable of resolution and accuracy of 2×10^{-3} mm. See A2.2 for details on deflection measurement and creep strain calculation.

6.6 *Data Acquisition*—Accurate determination of the time-to-failure (or maximum test time in case of run-out) is important, since time-to-failure is the only dependent variable in this test method. Applied force versus elapsed time shall be measured and recorded during testing to ensure constant stress conditions.

6.6.1 Accurate time determination is particularly important when time-to-failure may be relatively short (<10 s). Devices to measure time-to-failure may be either digital or analog and incorporate a switching mechanism to mark the time of test specimen failure. Either analog chart recorders or digital data acquisition systems may be used for this purpose.

6.6.2 Time recording devices shall be accurate to 1.0 % of the recording range and shall have a minimum data acquisition rate sufficient to adequately describe the whole test data series. The appropriate data acquisition rate depends on the actual time-to-failure but should preferably be in the 0.2 to 50 Hz range (50 Hz for times less than 5 s, 10 Hz for times between 5 s and 10 min, 1 Hz for times between 10 min and 5 h, and 0.2 Hz for times over 5 h).

6.7 *Dimension Measuring Devices*—Micrometers and other devices used for measuring test specimen dimensions shall have a resolution of 0.002 mm or smaller. To avoid damage in the inner span section, thickness/depth measurements should be made using a flat, anvil type micrometer. Ball-tipped or sharp anvil micrometers should not be used because localized surface damage (e.g., cracking) may be induced.

7. Test Specimen

7.1 *Specimen Size*—The types/configurations, dimensions, and tolerances of rectangular flexure beam specimens described in Test Method C1211 shall be used in this test method. The nominal dimensions [width (b), depth (d), and length (l)] for each type of test specimen are given in Table 1.

7.2 *Specimen Preparation*—Specimen fabrication and finishing methods as described in Test Method C1211, Section 7.2, shall be used in this test method. These methods are defined as application-matched machining, customary procedures, and standard procedures.

7.3 *Specimen Measurement*—It is common practice to measure the specimen dimensions post-test to prevent surface damage in the critical area (inner span section). If there is a concern about dimensional changes in test specimens from

TABLE 1 Test Specimen Dimensions (per Test Method C1211)^{A,B}

| Type/ Configuration | Width (b), mm | Depth/Thickness (d), mm | Length (l) mm, minimum |
|------------------------|----------------------|--------------------------------|-------------------------------|
| A | 2.0 | 1.5 | 25 |
| B | 4.0 | 3.0 | 45 |
| C | 8.0 | 6.0 | 90 |

^A Cross-sectional dimensional tolerances are ± 0.05 mm for A specimens and ± 0.13 mm for B and C specimens.

^B The parallelism tolerances on the four longitudinal faces are 0.015 mm for A and B specimens and 0.03 mm for C specimens. The two end faces need not be precision machined.

oxidation/reaction layers on the surface over long test times, measure the test specimen dimensions prior to testing.

7.3.1 For measurements prior to and after testing, determine the width (b) and depth (d) at three points along the inner span of each test specimen as described in Test Method C1211, either optically or mechanically using a flat, anvil-type micrometer. Exercise extreme care in pretest measurements to prevent damage to the critical area (the inner span section) of the test specimen. Record and report the measured dimensions and locations of the measurements. Use the average of the multiple measurements (width and depth) in the stress calculation.

7.3.2 Measurement of surface finish is not required, however, such information may be helpful in assessing surface flaws. Methods such as contact profilometry may be used to determine the surface roughness of the test specimen faces. When measured, report the measured surface roughness (RMS), test method, and the direction of the measurement with respect to the long axis of the test specimen.

7.4 Handling, Cleaning, and Storage—Exercise care in handling and storing specimens in order to avoid introducing random and severe flaws, which might occur if the specimens were allowed to impact or scratch each other. Clean the test specimens with an appropriate medium such as methanol or high-purity (> 99 %) isopropyl alcohol to avoid contamination of the test environment by residual machining or processing fluids. After cleaning and drying, store the test specimens in a controlled environment such as a vacuum or a desiccator in order to minimize exposure to moisture. Adsorbed moisture on the test specimen surfaces may change slow crack growth rates.

7.5 Number of Test Specimens—The required number of test specimens depends on the desired level of statistical reproducibility of the calculated SCG parameters (n and D). The statistical reproducibility is a function of the strength scatter number (Weibull modulus), the range of applied stress levels, and the SCG parameter (n). Because of these different variables, there is no absolute rule as to the determination of the appropriate number of test specimens.

7.5.1 A minimum of ten specimens per each applied stress level is recommended in this test method with at least four different applied stress levels (4 stresses \times 10 specimens = 40 specimens). The recommended number of test specimens (and applied stress levels) has been established with the intent of determining reasonable confidence limits on both time-to-failure distribution and SCG parameters. (See 8.1.1.)

NOTE 9—Refer to Ref 1 when a specific purpose is sought for the statistical reproducibility of SCG parameters.

7.6 Randomization of Test Specimens—Since a large number of test specimens (a recommended minimum of 40) with at least four different applied stresses is used in this test method, it is highly recommended that all the test specimens be randomized prior to testing in order to reduce any systematic error associated with material fabrication or specimen preparation, or both. Randomize the test specimens (using, for example, a random number generator) in groups equal to the number of applied stresses to be employed. Complete random-

ization may not be appropriate if the specimens are taken from different billets. Trace and record the source of the test specimens and use an appropriate statistical blocking scheme for distributing the specimens.

7.7 Valid Tests—A valid individual test is one that meets the following three requirements: (1) all the experimental requirements of this test method are met, (2) fracture occurs in the uniformly stressed section (that is, in the inner span; see 8.10.2), and (3) the maximum creep strain does not exceed the selected creep strain limit.

8. Procedure

8.1 Test Preparation:

8.1.1 Range and Number of Applied Stress Levels—The choice of range and number of applied stress levels (or applied force levels) not only depends on test material but also affects the statistical reproducibility of SCG parameters. A minimum of ten specimens per each applied stress level is recommended in this test method with at least four different applied stress levels (4 stresses \times 10 specimens = 40 specimens).

8.1.2 In general, choose an upper limit of applied stress that would result in a corresponding time-to-failure of ~ 10 s. The choice of the lower limit of applied stresses depends on run-out times, where some of the test specimens would not fail within a prescribed length of test time. Determine an appropriate run-out time for each particular test program, depending on the SCG mechanisms of the ceramic and the material service and temperature requirements. Reported laboratory tests of high strength, high temperature ceramics have used a range of run-out times: 10^6 , 10^7 , and 10^8 seconds. Choose at least four applied stresses covering at least four orders of magnitude in time.

NOTE 10—Time-to-failure of advanced monolithic ceramics in constant stress testing is probabilistic. Furthermore, the scatter in time-to-failure is significantly greater than the scatter in strengths (Refs 11-13), typically ($n+1$) times the Weibull modulus of strength distribution (see Appendix X2). Hence, unlike metallic or polymeric materials, a considerable increase in the scatter of time-to-failure is expected for advanced monolithic ceramics, attributed to both a large strength scatter (Weibull modulus of about 10 to 15) and a typically high SCG parameter $n \geq 20$. As a consequence, testing a few test specimens at each applied stress using a few stress levels may not be sufficient to produce statistically reliable design data. On the other side of the equation, the use of many test specimens with many applied stresses is quite time consuming and may be unrealistic in time and cost.

NOTE 11—If SCG parameters are available from constant stress-rate testing (Test Method C1368 and Test Method C1465), time-to-failure in constant stress testing can be estimated as a function of applied stress from a prediction shown in Appendix X3. This approach, although theoretical, allows one to quickly find the range and magnitude of stresses and the run-out time to be applied. There might be some discrepancies in the prediction; however, use of this prediction may significantly reduce many uncertainties and trial-and-errors associated with selecting stresses and run-out time. If no SCG data for the test material is available, run simplified constant stress-rate testing using both high (around 10 MPa/s) and low (around 0.01 MPa/s) stress rates with at least five test specimens at each stress rate to determine fracture strengths. Then determine the corresponding SCG parameters (n and D_0) based on the procedure in Test Method C1368. Use these simplified SCG data to select applied stresses and run-out time to be used in constant stress testing by following the prediction described in Appendix X3.

8.1.3 For each selected stress level, calculate the necessary applied force for the dimensions of the selected test specimen and loading configuration, using the stress calculation equation (Eq 1) in 9.1.1.

8.1.4 Define a heating rate for the furnace that will minimize temperature overshoot and thermal shock to the test specimen.

8.2 *Test Specimen Inspection and Measurement*—Conduct 100 % inspection of the test specimens to assure compliance with the specifications in this test method. Specimen dimensions (width, b , and depth, d) are commonly measured post-test, to prevent pretest damage to the surfaces of the test specimen (see 7.3.1 and 8.10.2). If there is a concern about a dimensional changes in test specimens from oxidation/reaction layers on the surface over long test times, measure the test specimen dimensions prior to testing.

8.3 *Test Fixture and System Assembly:*

8.3.1 *Test Fixtures*—Choose the appropriate fixture for the specific test configurations, as described in 6.2. Use the four-point “A” fixture for the Size A specimens. Similarly, use the four-point “B” fixture for Size B specimens, and the four-point “C” fixture for Size C specimens. Use a fully articulating fixture if the specimen parallelism requirements cannot be met.

8.3.2 *Inspecting and Assembling the Test Fixture*—Examine the bearing cylinders to make sure that they are undamaged, and that there are no reaction products (corrosion products or oxidation) that could result in uneven line loading of the test specimen or could prevent the bearing cylinders from rolling. Remove and clean, or replace, the bearing cylinders, if necessary. Avoid any undesirable dimensional changes in the bearing cylinders, for example, the inadvertent forming a small flat on the cylinder surface when abrasion (e.g., abrasive paper) is used to remove the reaction products from the cylinders. The same care should be directed toward the contact surfaces of the loading and support members of the test fixture that are in contact with the bearing cylinders. Assemble the test fixture, so that it is properly aligned and can articulate without restraint or significant friction.

8.3.3 *Furnace and Environmental Chamber Set Up*—Install and assemble the heating/furnace system (and environmental chamber, if used) so that it is properly aligned and functioning for test specimen heating, environmental control, and testing.

8.3.4 *Load System Set-Up*—Set up and check the load-control and force measurement devices in the test system. For dead weight systems, select and mount the required weights into the load train. For universal test machines, set the test mode to load-control.

8.4 *Test Specimen Loading and Heating:*

8.4.1 Carefully place the test specimen into the test fixture to avoid possible damage and contamination and to ensure alignment of the test specimen relative to the test fixture. There should be an equal amount of overhang of the test specimen beyond the outer bearing cylinders and the test specimen shall be directly centered below the axis of the applied force. Provide a method (e.g., pencil marking in the test specimen or known positioning of the test specimen relative to a reference point or surface of the test fixture) to determine the fracture location of the test specimen upon fracture.

8.4.2 *Loading the Test Fixture/Specimen Assembly into Test Machine*—Mount and align the test specimen/ fixture assembly in the load train of the test machine. If necessary, slowly apply a preload of no more than 25 % of the test force to maintain system alignment during deflection probe positioning and specimen heat up.

8.4.3 If test specimen deflection is to be measured (see 6.5) using a contact type of equipment, position the deflection-measurement probe(s) with its rounded tip in contact with the midpoint and/or the inner load points (tension side) of the test specimen. Exercise care to apply an appropriate contact force (see 6.5.2 and Annex A2).

8.5 An appropriate containment shield should be furnished for keeping test fragments from scattering in the furnace after fracture. If possible, retrieve the test specimens from the furnace as soon as possible after fracture in order to preserve the primary fracture surfaces for subsequent fractographic analysis.

8.6 *Environment*—Choose the test environment as appropriate to the test program. If the test environment is other than ambient air, supply the environmental chamber with the test atmosphere so that the test specimen is completely exposed to the test atmosphere. Consistent conditions (composition, supply rate, etc.) of the test environment should be maintained throughout the test series (see 6.4). If the tests are carried out in a humid atmosphere, the relative humidity should not vary more than 10 % (absolute) during the entire test series. At ambient temperatures, determine the relative humidity in accordance with Test Method E337. Allow a sufficient period for equilibration of the test specimen in the test environment.

8.7 *Heating to the Test Temperature*—Initiate the temperature data acquisition. Heat the test specimen to the test temperature at the selected heating rate. Temperature overshoot over the test temperature shall be strictly controlled and shall be no more than 5°C. Maintain the temperature within $\pm 5^\circ\text{C}$ (soak time) to allow the entire system to reach thermal equilibrium. Prior to testing, the soak time should be determined experimentally at the test temperature. The soak time shall be stated in the test report.

8.8 *Hot-Furnace Loading and Heating (Optional)*—In some cases, test specimens may be loaded directly into a hot furnace, as described in section 8.4 of Test Method C1211. The fixture may be either left in the furnace for the entire time or removed partially or completely, depending on the details of the system. Exercise care to ensure that the bearing cylinders and test specimen are positioned accurately. Furthermore, exercise extreme care to ensure that possible damage associated with thermal shock shall not have any effect on strength or slow crack growth, or both, of test specimens. If needed and possible, place the deflection-measurement probe in contact with the midpoint of specimens between the two inner bearing cylinders, in accordance with 8.4.3. Determine the equilibration time of the test specimen at the test temperature experimentally prior to testing.

8.9 *Conducting the Test*—Initiate the data acquisition for force, temperature, time, and deflection (if measured). Start the test by applying the selected applied force (applied stress) with

an accuracy of $\pm 1.0\%$ in a smooth, controlled manner. Time-measuring devices, particularly when used with dead-weight test machines, should be synchronized upon the application of a test force to the test specimen. Elapsed time shall be measured at an accuracy of $\pm 1\%$ of the actual value.

8.9.1 Recording—Record the force and temperature versus time data for each test in order to check the requirement for constant force and temperature during the test. Care should be taken to ensure adequate response-rate capacity of the recorder, as described in **6.6**. Upon specimen fracture or failure, record the time-to-failure for each test. If failure does not occur within the specified run-out time, record the elapsed time as a run-out.

8.9.2 If specimen deflection is measured during the test, record the deflection versus time data for each test.

8.9.2.1 Deflection Increases over Time in the Deflection-Time Plot—If the measured deflection increases over time at a constant force level (observed from the recorded deflection-time plot), creep strain/deformation is probably present (see **Fig. 3**). Creep strain may become dominant at higher test temperatures and longer test times. Although it is difficult to specify a general limit on maximum creep strain, it may be appropriate to limit the nominal (tensile face) creep strain to no more than 0.1% (Ref **16** and Test Method **C1465**). A larger or smaller creep strain limit may be defined, based on a mutual agreement, but this shall be stated in the report. If the maximum creep strain for a given stress level is greater than the agreed upon limit, use a higher applied stress while still meeting the requirement for at least four different applied stress levels.

8.10 Post-Test Treatments and Analysis:

8.10.1 After fracture, carefully collect as many test specimen sections and fragments as possible. Clean the sections and fragments if necessary and store in a protective container for further analysis, including fractography and creep deflection measurement.

8.10.2 Post-Test Specimen Dimensions—Measure and record the width (d) and depth (b) of each test specimen to within 0.002 mm , at one point near the fracture origin and two points near the load points. In the special case where there is a concern about dimensional change of test specimens after testing due to oxidation/reaction surface layers, take the measurements prior to testing (see **7.3**).

8.10.3 Fracture Location—Examine the location of fracture origin for each test specimen. Make certain that a valid test is one in which fracture occurs only in the uniformly stressed section (that is, the inner span).

NOTE 12—Due to the nonuniform, steep stress-gradients occurring in the sections outside the inner span, it is rarely possible to determine the exact stress level of a test specimen that fractured outside the inner span. Therefore, the test specimens that fractured outside the inner span are not recommended for use as valid data points in determining the slow crack growth parameters. In the case of multiple fractures, it is recommended to ascertain that the primary fracture occurred inside the inner span. Guidance for determining primary fracture is given in Practice **C1322**.

8.10.4 From a conservative standpoint, when completing a required number of test specimens at each stress level, test one replacement test specimen for each invalid test specimen (fracture outside the inner span or excessive creep deformation). If test specimens at a given stress level consistently have

excessive creep strain, perform tests at a higher stress level. However, for more rigorous statistical analysis (such as Weibull statistics) with a large number of test specimens, a censoring technique may be used to deal with such anomalous data points as discussed in Practice **C1239**.

8.10.5 Fractography—Fractographic analysis of fractured test specimens may be used to ensure that all the fracture origins are from the same population. Additional fractography may be performed to characterize the types, locations, and sizes of fracture origins as well as the flaw extensions due to slow crack growth. Fractography may also show signs of creep deformation. Follow the guidance established in Test Method **C1322**.

8.10.6 Creep deformation can be measured from retrieved test specimens, by measuring the permanent deformation at the midpoint of the test specimen by optical or mechanical dimension measurement. (See **A2.2.3**.)

9. Calculation

9.1 Applied Stress:

9.1.1 Calculate the applied flexural stress for each test specimen according to the elastic stress formula for a beam in four-point- $1/4$ point flexure:

$$\sigma = \frac{3PL}{4bd^2} \quad (1)$$

where:

σ = applied flexure stress, MPa,
 P = applied force, N,
 L = outer (support) span, mm,
 b = test specimen width, mm, and
 d = test specimen depth, mm.

9.1.2 Alternate Practice—**Eq 1** neglects to compensate for thermal expansion of the fixture and specimen at elevated test temperatures, since all dimensions are taken at room-temperature. Expansion of the fixture and specimen may lead to errors of 1 to 3 % for advanced ceramic materials such as alumina, silicon carbide, silicon nitride, and zirconia. Annex A1.1 in Test Method **C1211** provides a modified formula for **Eq 1** and shall be used if the average thermal expansion coefficient of the fixture and the specimen are known. The use of the thermal expansion corrected equations shall be stated explicitly in the report.

9.1.3 If the test specimens edges are chamfered or rounded, and if the sizes of the chamfers or rounds exceeds the limits in **7.2.4.8** and **Fig. 4** in Test Method **C1161**, then the strength of the beam shall be corrected in accordance with Annex A2 of Test Method **C1161**. The use of the chamfer corrected equations shall be stated explicitly in the report.

9.2 Determining the Constant Applied Stress versus Time-to-Failure Curve and the Slow Crack Growth Parameters n and D :

9.2.1 Individual time-to-failure test values for each test specimen (not the averaged time per applied stress), are used to determine the time-to-failure curve. This may be done by linear regression or maximum likelihood regression. If the data contains specimens that failed upon initial loading, a censored analysis shall be performed (left hand censoring); if the data

contains run-outs, a right hand censoring shall be performed. (See A1.3.) Datasets that contain both failures upon loading and run-outs shall be analyzed by a two-sided censoring technique. The censoring may be performed by an iterative least squares procedure or by a maximum likelihood analysis. Several commercial statistics analysis programs and certain freeware contain censored analyses as an analysis option (Refs 30-32).

9.2.2 Determination of SCG parameters depends on which crack velocity relationship is selected. The approach based on a power law relationship between crack velocity and applied stress intensity is given as the preferred method in this test method. See Appendix X1 for derivations and alternative methods.

9.2.3 Use the individual time-to-failure values t_f to determine the SCG parameters. Plot the log of the applied stress (σ in MPa) against the log of time-to-failure (t_f in s). The SCG parameters n and D_s may be determined by a linear regression analysis using all log t_f data over the complete range of individual log σ data, based on the following equation (see Appendix X1 for derivation):

$$\log t_f = -n \log \sigma + \log D_s \quad (2)$$

9.2.3.1 Include all the data points determined as valid tests in the diagram. However, do not include the run-outs or the data points in the plateau regions (see Fig. A1.1) in calculating SCG parameters. Examples of plots of log (*applied stress*) against log (*time-to-failure*) for two different ceramics at elevated temperatures are shown in Fig. 2.

NOTE 13—It seems to be more logical to plot the dependent variable, log (t_f), as a function of the independent variable, log (σ); however, it has been a long practice to plot log (σ) versus log (t_f) such as in Fig. 2. This type of diagram when determined under cyclic loading is called an *S-N* curve (E1823). This SCG test method follows this common convention in plotting data points. However, the regression shall be performed as defined in Eq 2.

NOTE 14—This test method is intended to determine only slow crack growth parameters n and D . The calculation of the parameter A (in $v = A[K_I/K_{IC}]^n$) requires knowledge of other material parameters, and is beyond the scope of this test method (see Appendix X1).

NOTE 15—This test method is primarily for test specimens with intrinsic flaws. If test specimens, however, possess any residual stresses produced by localized contact damage (e.g., particle impact or indents) or any other treatments, the estimated SCG parameters will be different and shall be denoted as such. Refer to Ref 33 for more detailed information on the analysis of slow crack growth behavior of a material containing a localized residual stress field.

9.2.4 Calculate the slope of the linear regression line as follows:

$$\alpha = \frac{K \sum_{j=1}^K (\log \sigma_j \log t_j) - \left(\sum_{j=1}^K \log \sigma_j \sum_{j=1}^K \log t_j \right)}{K \sum_{j=1}^K (\log \sigma_j)^2 - \left(\sum_{j=1}^K \log \sigma_j \right)^2} \quad (3)$$

where:

α = slope of the linear regression line,
 σ_j = the j th applied stress, MPa,
 t_j = the j th measured time-to-failure, s, and
 K = total number of test specimens tested validly for the whole series of tests excluding the plateau and run-out test specimens.

9.2.5 Calculate the SCG parameter n as follows:

$$n = -\alpha \quad (4)$$

9.2.6 Calculate the intercept of the linear regression line as follows:

$$\beta = \frac{\left(\sum_{j=1}^K \log t_j \right) \sum_{j=1}^K (\log \sigma_j)^2 - \left(\sum_{j=1}^K \log \sigma_j \log t_j \right) \left(\sum_{j=1}^K \log \sigma_j \right)}{K \sum_{j=1}^K (\log \sigma_j)^2 - \left(\sum_{j=1}^K \log \sigma_j \right)^2} \quad (5)$$

where:

β = zero intercept of the linear regression line.

9.2.7 Calculate the SCG parameter D_s as follows:

$$D_s = 10^\beta \quad (6)$$

9.2.8 Calculate the standard deviations of the slope α and of the SCG parameter n as follows:

$$SD_\alpha = \sqrt{\frac{K \sum_{j=1}^K (\alpha \log \sigma_j + \beta - \log t_j)^2}{K-2 \left[K \sum_{j=1}^K (\log \sigma_j)^2 - \left(\sum_{j=1}^K \log \sigma_j \right)^2 \right]}} \quad (7)$$

$$SD_n = SD_\alpha \quad (8)$$

where:

SD_n = standard deviation of the SCG parameter n , and
 SD_α = standard deviation of the slope, α .

9.2.9 Calculate the standard deviations of the intercept β and of the SCG parameter D_s as follows:

$$SD_\beta = \sqrt{\frac{\sum_{j=1}^K (\alpha \log \sigma_j + \beta - \log t_j)^2 \sum_{j=1}^K (\log \sigma_j)^2}{(K-2) \left[K \sum_{j=1}^K (\log \sigma_j)^2 - \left(\sum_{j=1}^K \log \sigma_j \right)^2 \right]}} \quad (9)$$

$$SD_{D_s} = 2.3026 (SD_\beta) (10^\beta) \quad (10)$$

where:

SD_β = standard deviation of the intercept β , and
 SD_{D_s} = standard deviation of the SCG parameter D_s .

9.2.10 Calculate the coefficients of variation of the SCG parameter n and of the SCG parameter D_s as follows:

$$CV_n(\%) = \frac{100(SD_n)}{n} \quad (11)$$

$$CV_{D_s}(\%) = \frac{100(SD_{D_s})}{D_s} \quad (12)$$

where:

CV_n = coefficient of variation of the SCG parameter n , and
 CV_{D_s} = coefficient of variation of the SCG parameter D_s .

9.2.11 Calculate the square of the correlation coefficient (r^2) of the linear regression line as follows:

$$r^2 = \frac{\left[K \sum_{j=1}^K (\log \sigma_j \log t_j) - \left(\sum_{j=1}^K \log \sigma_j \sum_{j=1}^K \log t_j \right) \right]^2}{\left[K \sum_{j=1}^K (\log \sigma_j)^2 - \left(\sum_{j=1}^K \log \sigma_j \right)^2 \right] \left[K \sum_{j=1}^K (\log t_j)^2 - \left(\sum_{j=1}^K \log t_j \right)^2 \right]} \quad (13)$$

where:

r^2 = square of the correlation coefficient.

9.2.12 *Optional*—The mean time-to-failure is not used in this method to calculate SCG parameters. If desired for a specific purpose, calculate for each applied stress the corresponding mean time-to-failure with standard deviation and coefficient of variation as follows:

$$\bar{t}_f = \frac{\sum_{j=1}^N t_j}{N} \quad (14)$$

$$SD_{t_f} = \sqrt{\frac{\sum_{j=1}^N (t_j - \bar{t}_f)^2}{N - 1}} \quad (15)$$

$$CV_{t_f}(\%) = \frac{100(SD_{t_f})}{\bar{t}_f} \quad (16)$$

where:

\bar{t}_f = mean time-to-failure, s,

t_j = the j th measured time-to-failure value, s, for each applied stress,

N = number of test specimens tested validly at each applied stress, excluding the run-out specimens and specimens that failed upon initial loading; when there is no run-out test specimen, the minimum number of test specimens is 10,

SD_{t_f} = standard deviation, and

CV_{t_f} = coefficient of variation.

9.3 If creep deformation is measured during or after the test, calculate the creep strain per Annex A2.2.4.

10. Report

10.1 *Test Specimens, Equipments, and Test Conditions*—Report the following information for the test specimens, equipment, and test conditions. Note in the report any deviations and alterations from the procedures and requirements described in this test method.

10.1.1 Date and location of the testing.

10.1.2 Specimen geometry description and specimen dimensions. Include if the specimen has chamfered or rounded edges with dimensions.

10.1.3 The number of test specimens tested at each applied stress level.

10.1.4 All relevant material data including vintage data or billet identification data.

10.1.5 Exact method of test specimen preparation, including all stages of machining.

10.1.6 Heat treatments or heat exposures, if any.

10.1.7 Relevant information on randomization of the test specimens.

10.1.8 Methods of test specimen cleaning and storage.

10.1.9 All preconditioning of test specimens prior to testing, if any.

10.1.10 Type and configuration of the test machine including the loading method and control and the force measurement system.

10.1.11 Type, configuration, dimensions (inner and outer span), and material of the test fixture with the degree of articulation. A diagram of the test fixture is recommended.

10.1.12 Type and configuration of the data acquisition system.

10.1.13 Type and configuration of the heating system—furnace configuration and thermal control.

10.1.14 Type and configuration of the temperature measurement system.

10.1.15 If used, the type and configuration of the environmental chamber and control system and environmental test conditions.

10.1.16 If used, the type and configuration of the specimen deflection and creep deformation measurement system.

10.1.17 If used, the method of post-test measurement of the permanent creep deformation and calculation of the creep strain.

10.1.18 Ambient conditions such as temperature and humidity.

10.1.19 Method and magnitude of preloading for each test specimen, if any.

10.1.20 Number and magnitude of applied forces (in N) and stresses (in MPa) and test temperatures (°C) in the test sequence.

10.1.21 Defined run-out time limit in seconds.

10.1.22 Defined maximum creep strain limit in mm/mm and %.

10.1.23 Measured furnace “soak” time for specimen thermal equilibrium.

10.2 *Test Results*—Report the following information for the test results. Note in the report any deviations and alterations from the procedures and requirements described in this test method.

10.2.1 Number of the valid tests, (e.g., fracture in the inner span and minimal creep strain) as well as the number of invalid tests (e.g. fracture outside the inner span and/or excessive creep strain).

10.2.2 Equations used for flexure stress calculation and whether the thermal expansion corrections for the fixtures and specimen and the chamfer corrections were used.

10.2.3 For each test specimen, measured dimensions (b and d to an accuracy of 0.002 mm), test temperature to an accuracy of $\pm 5^\circ\text{C}$, and applied force (in Newtons to three significant figures).

10.2.4 For each test specimen, the calculated stress in MPa to three significant figures and the time-to-failure (or run-out time) of each test specimen in seconds (to three significant figures).

10.2.5 Mean time-to-failure with standard deviation, and coefficient of variation determined at each applied stress and each test temperature, if determined (optional).

10.2.6 For the test data set at a given test temperature, the calculated values for the SCG parameters n and D_s with the standard deviations (SD) and coefficients of variation (CV) for n and D_s , and the square of the correlation coefficient (r^2).

10.2.7 Graphical representation (see Fig. 2) of the test results showing log (applied stress) against log (time-to-failure) using all data points including the run-outs. Include in

the figure the determined best-fit line together with the estimated value of SCG parameters n and D_S . Include in the figure, if desired, key information on test material, test temperature, and test environment, etc., as shown in Fig. 2.

10.2.8 If measured, the calculated creep strain for individual test specimens.

10.2.9 If measured, the measured surface roughness (RMS), test method, and the direction of the measurement.

10.2.10 Fractography information including type, location and size of fracture origin as well as the degree of slow crack growth, if possible.

11. Precision and Bias

11.1 The time-to-failure of an advanced ceramic for a given applied stress is not a deterministic quantity, but will vary from test specimen to test specimen. Weibull statistics, as discussed in Practice C1239, may model this variability (Refs 3, 12, 13, 34). This test method has been devised so that the precision is high and the bias is low compared to the inherent variability of time-to-failure of the material.

11.2 The experimental stress errors, as well as the error due to cross-section reduction associated with chamfering the edges, have been analyzed in detail in Ref 4 and described in

terms of precision and bias in Test Method C1211. Test Method C1211 also includes chamfer correction factors that shall be used if necessary.

11.3 The statistical reproducibility of slow crack growth parameters determined from constant stress testing has been analyzed (Ref 1). The degree of reproducibility of SCG parameters depends on not only the number of test specimens but also on other experimental test variables. These variables include the SCG parameters, Weibull modulus, the number and range of test stresses, and the test temperatures.

11.4 Bias may result from inadequate use or treatments, or both, of the test environment, particularly in terms of its composition, aging, and contamination.

11.5 Because of the nature of the materials and the lack of a wide database on a variety of applicable advanced ceramics tested in constant stress testing, no definitive statement can be made at this time concerning precision and bias of this test method.

12. Keywords

12.1 advanced ceramics; constant stress testing; elevated temperature; flexural testing; four-point flexure; slow crack growth; slow crack growth parameters; time-to-failure

ANNEXES

(Mandatory Information)

A1. INTERFERENCES

A1.1 At elevated temperatures, significant creep strain and damage (in the form of creep cavities, micro- or macro-cracks, or both) may develop on or near the tensile surface at higher temperatures (Ref 16-18, 35). That damage may produce two interferences: (1) reduced strength because of crack growth based on cavitation and microcracking and (2) nonlinearity in stress-strain relations based on accumulated damage on the tensile face in flexure (Ref 35). It has been reported that the strength degradation with respect to the expected normal strength ranged from 15 to 50 % (Refs 16-19, 23-27).

NOTE A1.1—Elevated temperature creep testing and creep stress rupture testing of monolithic ceramics are addressed in C1291.

A1.2 If creep occurs at elevated temperatures, the maximum stress on the outer fiber surface (the outer face of the flexure beam) decreases, the neutral axis shifts, and the stress profile is no longer linear. This effect, depending on the degree of nonlinearity, may limit the applicability of linear elastic fracture mechanics (LEFM), since the resulting relationship between strength and stress rate derived under constant stress testing condition is based on an LEFM approach with negligible creep (Ref 36).

A1.2.1 Therefore, creep strain should be kept as minimal as possible (to no more than 0.1 %), as compared to the total elastic strain at failure (see 8.9.2).

A1.3 Depending on the degree of SCG susceptibility of a material, the linear relationship between log (*constant applied stress*) and log (*time-to-failure*) may start to deviate at a certain high applied stress levels where the crack velocity increases rapidly with a subsequently short test duration, i.e., conditions when the applied stress approaches the ultimate flexural strength (see Fig. A1.1). This is analogous to the occurrence of a strength plateau observed at higher test rates in constant stress-rate testing (Ref 37). If the time-to-failure data determined in this plateau region are included in the analysis, a misleading estimate of the SCG parameters will be obtained (Ref 38). Therefore, the strength data in the plateau shall be censored/excluded as data points in estimating the SCG parameters of the material. Similarly, one or more run-out data points may also exist at the low-stress, long time-to-failure end of the curve, and these run-out data points shall be censored/excluded in estimating the SCG parameters (see Fig. A1.1).

NOTE A1.2—There are no simple guidelines in determining whether a plateau region is reached; however, with knowledge of the inert strength and the fracture toughness of the test material, the slow crack growth rate—applied stress intensity (v-K) curve may be determined. Evaluating this will help determine where the experimental conditions fall.

A1.4 *Crack Healing*—Oxidation-induced crack healing or crack tip blunting at elevated temperatures (which dominates slow crack growth) may produce an appreciable increase in

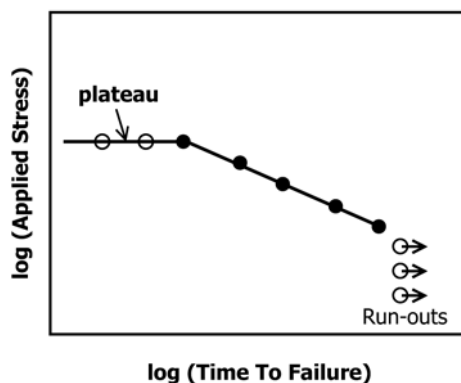


FIG. A1.1 Schematic Diagram Showing Unacceptable (Average) Data Points (With an “Open” Symbol) in the Plateau Region and Run-out Data Points (symbol with arrows) at Low Stresses in Determining Slow Crack Growth (SCG) Parameters

time-to-failure for some ceramics. It has been reported that the crack healing produced significant increases in fast-fracture strength and longer time-to-failures for a given applied stress for silicon nitride, mullite-SiC, and alumina. (Refs [16](#), [39](#), [40](#)). Since the phenomenon results in a deviation from the linear relationship between log (flexural strength) and log (time-to-failure), an overestimate of SCG parameters may be obtained if such anomalous time-to-failure data are included in the analysis. Therefore, any data exhibiting a significant or obvious increase in time-to-failure at lower stress levels shall be excluded as data points in estimating the SCG parameters of the material.

A1.5 When testing a material exhibiting a high SCG resistance (typically SCG parameter $n > 70$) an unrealistically large number of test specimens may be required in a small range of applied stresses since a significant number of test specimens may be expected to fail while loading. Furthermore, if lower stresses are to be used, unrealistically long test times are to be expected. As a result, practical, specific, quantitative values of SCG parameters required for life prediction can only be determined with great difficulty for this type of material (Ref [41](#)). In this case, a companion test method (constant stress-rate testing, Test Method [C1465](#)) may be utilized instead to determine the corresponding SCG parameters of the material. The constant stress-rate test may be used, provided the same flaw types are activated in both stress states.

A1.6 Ceramic test specimens may have a wide range of and variability in flaw populations that will effect the fracture strength.

A1.6.1 Test-specimen fabrication history may play an important role in strength as well as time-to-failure behavior, which consequently may affect the values of the SCG parameters to be determined. Therefore, the test specimen fabrication history shall be reported.

A1.6.2 Surface machining and grinding of test specimens may introduce anomalous surface flaws that may have pronounced effects on flexural strength and thus time-to-failure. Machining damage imposed during test specimen preparation can be either a random interfering factor, or an inherent part of the strength characteristics to be measured. Surface preparation may also lead to residual stress. It should be understood that

the final machining steps may or may not negate machining damage introduced during the earlier coarse or intermediate machining steps. In some cases, test specimens need to be tested in the as-processed condition to simulate a specific service condition.

A1.6.3 Surface flaws introduced while handling the specimens (e.g., scratches, edge chips) may produce premature fracture.

A1.7 The fabrication process used for certain advanced ceramic components may require testing of specimens with surfaces in the as-fabricated, non-uniform condition (i.e., it may not be possible, desired, or required to machine some test specimens directly in contact with test fixture components). In such cases, a fully articulated test fixture is required. In addition, for very rough or wavy as-fabricated surfaces, eccentricities in the stress state due to non-symmetric cross-sections as well as variations in the cross-sectional dimensions may also interfere with the strength measurement.

A1.8 Fractures that consistently initiate near the load pins may be due to factors such as friction or contact stresses introduced by the load fixtures or by misalignment of the test specimen load pins. Consistent failure of test specimens at their edges may be due to poor specimen preparation (e.g., severe grinding or very poor edge preparation) or excessive twisting stresses at the specimen edges (Refs [4](#), [5](#), [42](#)).

A1.9 Fractures may initiate from different flaw types (e.g., surface flaws—like scratches and machining flaws—or pores and agglomerates that may be located in the volume or at the surface of the specimens.) The analysis performed in this test method assumes that all failures initiate from similar types of flaws and should be confirmed by fractography in accordance with Test Method [C1322](#).

A1.10 Some high strength, high temperature ceramics (silicon nitride, aluminum oxide, etc.) have grain boundary and matrix phases which can oxidize, react, or crystallize (devitrify) at elevated temperatures and extended times. The modified grain boundaries and matrix phases may have different fracture properties, modified slow crack growth rates, and different creep rates, compared to the initial as-fabricated condition. Oxidation, reaction, and crystallization of internal

phases should be considered as a possible experimental variable and analyzed, as necessary, before and after the test.

A2. DIRECTIONS FOR EQUIPMENT AND TEST PROCEDURES

A2.1 System Compliance—For universal test machines the compliance of the load train shall be characterized for the loading range used and the testing temperature. The load train and fixtures shall be sufficiently rigid so that at least 80 % of the crosshead motion is transmitted to the actual test specimens. The load train and fixtures shall not permanently deform during testing. It is not necessary to check the system compliance for every test sequence, provided that it has been characterized previously for the identical setup.

A2.1.1 Compliance of the test fixture and load train at the test temperature can be estimated by inserting a rigid block of a ceramic material onto the test fixture with the load-bearing cylinders in place, and loading it to the maximum anticipated fracture force while recording a force-deflection curve. The compliance corresponds to the inverse of the slope of the force-deflection curve. It is recommended that the block be at least five times thicker than the test specimen depth and one to two times wider than the test specimen width. Any other block whose rigidity (equal to the inverse of compliance) is greater than at least 120 times that of the test specimen can be used provided that it can fit the test fixture. A typical test machine equipped with common load train and test fixtures shows that more than 90 % of the total compliance stems from the test specimen itself, so that more than 90 % of crosshead or actuator movement of the test machine can be imposed on the test specimen.

A2.2 Creep Deformation and Deflection Measurement—Increasing deflection and bending of the flexure test specimen over time under constant force is an indicator of possible creep deformation (see Fig. 3). This creep deflection of the test specimen can be measured at the midpoint or at the inner load

point(s) (tension side) of the test specimen during the test or post test (see Fig. A2.1).

A2.2.1 Beam Deflection by Contact Probe—Deflection of the test specimen may be measured by contact probes using LVDT transducers. Deflection may be measured on the tensile face of the test specimen at the specimen midpoint or under one of the inner load points. (See Fig. A2.1.) The relative deflection between the midpoint and the load points on the test specimen can also be measured using a three-probe configuration. Using three probes to measure relative deflection eliminates thermal effects on the displacement transducers.

A2.2.1.1 If a displacement transducer/s is used to measure the beam deflection during the test, the transducer shall have sufficient range to measure the full deflection of the test beam at maximum force. The transducer resolution shall be at least 0.002 mm for any displacement. The displacement transducer shall be calibrated. A contact-based linearly variable differential transformer (LVDT) is suitable for this purpose but any device (optical, capacitive, or other) may be used, provided that deflections of the beam are reliably measured as specified across the full range of test temperatures.

A2.2.1.2 When a contact-type deflection-measuring device is employed, it is important not to damage the contact surface of the specimens due to prolonged contact with the deflection-measuring probe, particularly at longer test times and higher test temperatures. Any spurious damage may act as a failure-originating source, so that the contacting force should be kept minimal, in the range from 0.5 to 2 N. A general guideline is that the maximum contacting force is dependent on specimen size, i.e., 0.5 N for Size A, 1 N for Size B, and 2 N for Size C

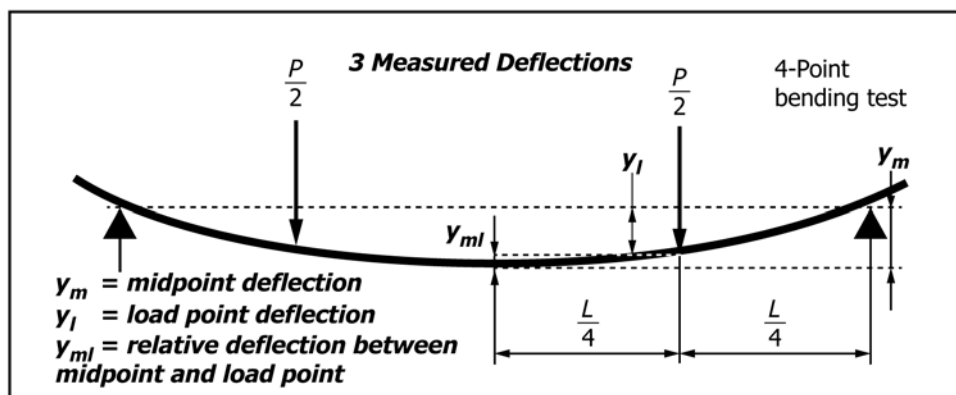


FIG. A2.1 Measured Beam Deflections

specimens. The probe with a rounded tip may be fabricated with the same material as the test specimens or with sintered silicon carbide.

A2.2.2 Deflection by Cross-head Displacement—Alternatively crosshead or actuator displacement may be used to infer deflection under the load point of the test specimen. However, care should be taken in interpreting the result since crosshead or actuator displacement generally may not be as accurate and as sensitive as deflection measurements taken on the specimen itself.

A2.2.3 Post Test Measurement of Permanent Center Point Deflection—By definition, creep deformation is permanent deformation which remains after the applied force is removed. After testing, unbroken and broken test specimens with creep deformation will have permanent bending deformation which can be measured by a suitable means. Measure the midpoint deflection relative to the deflection at the outer support points or to the inner loading points. This measurement of the midpoint deflection may be done by two methods: macropho-

tograph the test specimen and measure the deflection off of the photograph or use mechanical coordinate measuring contact probes.

A2.2.4 The maximum creep strain on the outer tensile surface for 4-point- $\frac{1}{4}$ point flexure is calculated using the linear elastic stress-strain equations for flexure beams (from Test Method **C1465**).

$$\epsilon_c = (A d \Delta y_x) / L^2 \quad (\text{A2.1})$$

where:

- ϵ_c = the maximum creep strain (mm/mm), (convert to a percentage by multiplying by 100),
- A = geometry factor—4.36 for midpoint deflection (y_m), 6.00 for load point deflection (y_l), and 16.0 for relative midpoint-load point deflection (y_{ml}),
- d = the test specimen depth/thickness, mm,
- Δy_x = the measured creep deflection, mm, for midpoint (y_m), load point (y_l), and relative midpoint-load point deflection (y_{ml}), and
- L = the outer/support span, mm.

APPENDIXES

(Nonmandatory Information)

X1. TIME-TO-FAILURE AS A FUNCTION OF APPLIED STRESS IN CONSTANT STRESS (“STATIC FATIGUE”) TESTING

X1.1 The SCG behavior of glass and ceramics can be described in terms of nominal v - K diagrams, which establish the relationship between the applied stress intensity, K , and the growth velocity of cracks, v , in a given environment (Ref **43**). If the v - K curve is known, lifetime prediction can be made through the use of fracture mechanics. Some materials may not exhibit a threshold stress intensity (K_{th}) below which no SCG occurs, whereas others may not have measurable stage II or III regimes before fast fracture occurs. In determination of the SCG parameters for material comparison and life time predictions, it is therefore imperative to establish the entire v - K curve rather than to just determine the slope, n , for stage I (Ref **44**). Several test methods assumes *a priori* knowledge of the v - K relationship, and much research has been focused on exploring the fundamental mechanisms governing subcritical crack growth behavior to establish a universal relationship between crack growth and applied stress intensity. Other test methods involve a direct measurement of the growing crack as a function of a well defined applied K , and hence, no assumptions on the functional relationship need to be made.

X1.2 Fracture Mechanics Equations:

X1.2.1 The Mode I stress intensity factor, K_{Ia} , for a flaw of size a (a represents the depth of a surface flaw or radius of a volume flaw) subjected to a remote applied stress of σ_a is given by:

$$K_{Ia} = Y \sigma_a \sqrt{a} \quad (\text{X1.1})$$

where Y is a crack geometry factor dependent on the flaw shape (Ref **45**). By rearranging and differentiating with respect

to time, the relationship between the applied stress (or stress intensity) and the change in crack size (crack velocity) may be obtained:

$$v = \frac{da}{dt} = \frac{2K_{Ia}}{Y^2 \sigma_a^2} \frac{dK_{Ia}}{dt} - \frac{2K_{Ia}^2}{Y^2 \sigma_a^3} \frac{d\sigma_a}{dt} \quad (\text{X1.2})$$

X1.2.2 In order to integrate Eq **X1.2** and obtain the strength in the degrading environment, an assumption of the relationship between the crack velocity v and the applied stress intensity K_{Ia} must be made.

X1.3 Power Law Formulation:

X1.3.1 The relationship most commonly used is a power-law representation and this is recommended as the preferred method in this test method. This approach introduces mathematical simplicity, and has been shown to empirically fit most SCG data well (Refs **2, 43, 46, 47**). The power law has also been adopted in several design codes for advanced ceramics. The crack velocity during sub-critical crack growth is given as:

$$v = A \left(\frac{K_{Ia}}{K_{IC}} \right)^n \quad (\text{X1.3})$$

X1.3.2 The constants A and n are the SCG parameters, dependent on material and environment, and K_{IC} is the material's Mode I plane strain fracture toughness. Often it is observed that the SCG behavior is temperature-dependent, and the power-law relationship may be modified to take this into account by introducing a term containing temperature-dependence:

$$v = v_0' \left(\frac{K_{Ia}}{K_{IC}} \right)^n \exp \left[- \left(\frac{E^*}{RT} \right) \right], \quad (X1.4)$$

where:

v_0' and n = the SCG parameters,
 E^* = the activation energy,
 R = the gas constant, and
 T = absolute temperature.

X1.3.3 The strength σ_i in the inert environment and σ_f in the strength reducing environment are given by:

$$K_{IC} = Y \sigma_i \sqrt{a_i} \quad (X1.5)$$

and

$$K_{IC} = Y \sigma_f \sqrt{a_f} \quad (X1.6)$$

respectively, with a_i and a_f representing the initial and final crack lengths. Using the power-law relation in Eq X1.3 in Eq X1.2 and utilizing the expressions in Eq X1.5, the following expression for the reduced SCG strength (σ_f) as a function of applied stress is obtained:

$$\sigma_f^{n-2} = \sigma_i^{n-2} - \frac{1}{B} \int_0^t [\sigma_a(t)]^n dt \quad (X1.7)$$

where:

$$B = \frac{2K_{IC}^2}{v_0 Y^2 (n-2)} \quad (X1.8)$$

X1.3.4 In the case of constant stress σ_a , Eq X1.6 may be integrated to determine the time-to-failure:

$$t_f = B \sigma_f^{-n} (\sigma_i^{n-2} - \sigma_f^{n-2}) \quad (X1.9)$$

and this may be further simplified to:

$$t_f = B \sigma_i^{n-2} \sigma_f^{-n} \quad (X1.10)$$

under the assumption that $\sigma_i / \sigma_f \gg 1$ (i.e., that the inert strength is much higher than the strength in a corrosive environment). Rearranging and taking logarithms, it is found that:

$$\log t_f = -n \log \sigma_f + \log B + (n-2) \log \sigma_i \quad (X1.11)$$

or simplified to Eq X1.12:

$$\log t_f = -n \log \sigma_f + \log D_s \quad (X1.12)$$

NOTE X1.1—For constant stress testing σ_f is identical to σ (the applied stress at failure), and these are used interchangeably.

X1.3.5 The SCG parameters n and D_s may be obtained from the slope and intercept of the failure time as a function of SCG strength in a log-log plot. For comparing various materials and conditions, Eq X1.11 is often rearranged in the following way (Ref 48):

$$\log(t \sigma_f^2) = \log B + (n-2) \log \left(\frac{\sigma_i}{\sigma_f} \right) \quad (X1.13)$$

X1.3.6 Similarly the modified power law Eq X1.4 can be used to yield the following expression for the time-to-failure:

$$t_f = \left(\frac{2}{AY^n(n-2)} \right) \sigma_f^{-n} a_i^{-\frac{2-n}{2}} \exp \left(- \frac{E^*}{RT} \right) \quad (X1.14)$$

X1.3.7 Taking logarithms and rearranging, Eq X1.14 may be used to determine the SCG parameter n . Notice that in this

formulation the intercept determined by regression analysis will contain different parameters than the D_s determined above.

X1.4 Exponential v - K Relationship:

X1.4.1 Alternatively an exponential relationship between v and K , which is easier to reconcile with fundamental aspects of SCG is given by (Ref 49):

$$v = A \exp \left[n \left(\frac{K_{Ia}}{K_{IC}} \right) \right] \quad (X1.15)$$

or in a more detailed version (Ref 50):

$$v = a' \exp \left(\frac{-E^*}{RT} \right) \exp \left(\frac{b K_{Ia}}{RT} \right) \quad (X1.16)$$

where a' , and b are the material-dependent SCG parameters.

X1.4.2 The necessary time-to-failure equations may be developed using this exponential relationship (Ref 50). For the constant stress case, the resulting equation is:

$$t_f = \left(\frac{2a}{K_i^2 a'} \right) \exp \left(\frac{-E^*}{RT} \right) \int_{K_i}^{K_{Ia}} K_{Ia} \exp \left(\frac{-b K_{Ia}}{RT} \right) dK \quad (X1.17)$$

where a' and b are the SCG parameters previously defined, a is the final crack length, and K_i is the initial stress intensity factor calculated from the initial crack length and applied force (Ref 48). The necessary time-to-failure equations may be developed using numerical solutions of these exponential relationships (Ref 29). The resulting time to failure for the crack velocity expression of Eq X1.15 is:

$$\ln t_f = - \left[\frac{n}{\sigma_i} \right] \sigma_a + \chi \quad (X1.18)$$

where $\chi = \ln \frac{a_i}{A} + \beta$ with β being a weak function of n .

X1.4.3 In the same way, the resulting time-to-failure for the crack velocity equation of Eq X1.16 is:

$$\ln t_f = - \left[\frac{b}{RT \sigma_i} \right] \sigma_a + \chi' \quad (X1.19)$$

where:

$$\chi' = \ln \left[\frac{a_i}{a'} \right] + \frac{E^*}{RT} + \beta \quad (X1.20)$$

X1.4.4 Therefore, SCG parameters can be conveniently determined from slope and intercept through a linear regression analysis of $\ln t_f$ versus σ_a together with known parameters. However, the above approach requires that the inert strength be known *priori* to determine the major SCG parameter n or b (see Eq X1.17 or Eq X1.18), which is a significant drawback as compared with the power-law formulation (Ref 50).

X1.5 No *a-priori* Assumption of the v - K Relationship:

X1.5.1 Gupta, et al., (Ref 51) citing early unpublished work by Fuller, presented an analysis deriving the v - K relationship from the applied stress and the time-to-failure without any prior assumption on the functional form. The approach was necessitated for the extrapolation of constant stress data for optical glass fibers into a region of long failure times or low stresses, in which the power law and the exponential law diverge by several orders of magnitude (Ref 20).

X1.5.2 Acknowledging this analysis, Eq X1.2 may be rewritten as:

$$\frac{dt}{dK} = \frac{K_{Ia}}{(Y \sigma)^2 v} \quad (X1.21)$$

and the time-to-failure can be determined as:

$$t_f = \left(\frac{2}{(Y \sigma)^2} \right) \int_{K_i}^{K_{Ic}} \left(\frac{K}{v} \right) dK \quad (X1.22)$$

X1.5.3 Gupta, et al. obtained $v(K)$ by taking the partial derivative of this expression with respect to K_i at fixed a_i , with the result being:

$$v(K_i) = \frac{\left[\frac{-2}{t_f} \right] \left[\frac{K_{Ic}}{Y \sigma_i} \right]^2}{2 + \frac{d(\ln t_f)}{d(\ln \sigma_f)}} \quad (X1.23)$$

X1.5.4 This approach requires the measurement of the inert strength and the fracture toughness, and then applying these the crack velocity v can be obtained for measuring the time-to-failure at different applied stresses.

X2. ESTIMATION OF SCATTER IN TIME-TO-FAILURE IN CONSTANT STRESS (“STATIC FATIGUE”) TESTING WITH RESPECT TO ESTIMATED SCATTER IN STRENGTH IN CONSTANT STRESS-RATE (“DYNAMIC FATIGUE”) TESTING (Refs 1-3)

X2.1 Strength distribution of most advanced ceramics can be described typically with the two-parameter Weibull function as follows:

$$\ln \ln \frac{1}{1-F} = m \ln \sigma_f - m \ln \sigma_o \quad (X2.1)$$

where:

- F = failure probability,
- m = Weibull modulus,
- σ_f = fracture strength, and
- σ_o = characteristic strength.

X2.2 Solving for $\ln \sigma_i$ in Eq X2.1 with $\sigma_f \equiv \sigma_i$ (for inert flexural strength) and substituting into Eq X1.11 after taking natural logarithms of both sides of Eq X1.11 yields:

$$\ln \ln \frac{1}{1-F} = \left[\frac{m}{n-2} \right] \ln t_f - \frac{m}{n-2} \ln [B \sigma_o^{n-2} \sigma^{-n}] \quad (X2.2)$$

X2.3 In the same way, for constant stress-rate testing, solving for $\ln \sigma_i$ with $\sigma_f \equiv \sigma_i$ (for inert strength) the following equation is obtained:

$$\ln \ln \frac{1}{1-F} = \left[\frac{m(n+1)}{n-2} \right] \ln \sigma_f - \frac{m(n+1)}{n-2} \ln [B (n+1) \sigma_o^{n-2} \sigma]^{-\frac{1}{n+1}} \quad (X2.3)$$

X2.4 Therefore, both the equivalent Weibull modulus (m_{es}) of the plot of failure probability versus time-to-failure in constant stress testing (Eq X2.2) and the equivalent Weibull modulus (m_{ed}) of the plot of failure probability versus fracture strength in constant stress-rate testing (Eq X2.3) are:

$$m_{es} = \frac{m}{n-2}; m_{ed} = \frac{m(n+1)}{n-2} \quad (X2.4)$$

X2.5 Therefore, from the equivalent Weibull moduli of Eq X2.2, a relationship can be found:

$$\frac{m_{es}}{m_{ed}} = \frac{1}{n+1} \quad (X2.5)$$

X2.6 Therefore, equivalent Weibull modulus of time-to-failure in constant stress testing is expected to be $1/(n+1)$ times that of fracture strength in constant stress-rate testing. In other words, for a given material/environment the scatter in time-to-failure would be $(n+1)$ times greater than the scatter (typically $m = 10$ to 15 for most advanced ceramics) in fracture strength. The scatter in time-to-failure would be significantly amplified since the SCG parameter n is typically greater than 20 for most advanced ceramics. The relation of Eq X2.5 thus verifies that a significant variation in time-to-failure is exacerbated in constant stress testing for advanced monolithic ceramics, as observed experimentally.

X3. A SIMPLIFIED PREDICTION OF TIME-TO-FAILURE IN CONSTANT STRESS (“STATIC FATIGUE”) TESTING BASED ON SCG DATA OBTAINED FROM CONSTANT STRESS-RATE (“DYNAMIC FATIGUE”) TESTING

X3.1 In this appendix, a simplified prediction of time-to-failure as a function of applied stress in constant stress testing is made based on the SCG data determined from constant stress-rate testing. This prediction, although theoretical, allows one to determine an approximate relationship between time-to-failure and applied stresses so that the range and number of applied stresses can be quickly and reasonably-well selected together with to-be-prescribed run-out times.

X3.2 From constant stress rate (dynamic fatigue) testing it was obtained (see Test Method C1368):

$$B\sigma_i^{n-2} = \frac{D_d^{n+1}}{n+1} \quad (\text{X3.1})$$

X3.3 Substitute Eq X3.1 into the time-to-failure (t_{fs}) equation to yield:

$$t_f = \left[\frac{D_d^{n+1}}{n+1} \right] \sigma^{-n} \quad (\text{X3.2})$$

where:

$$\log D_d = \log(B \sigma_i^{n-2}) \quad (\text{X3.3})$$

X3.4 Therefore, from the relationship in Eq X3.2, once the parameters n and D_d of a test material for a given environment are known from constant stress-rate testing, time-to-failure in constant stress testing may be easily estimated as a function of stress to be applied in the same environment. It would be more convenient to use Eq X3.2 if the equation is plotted. There might be some discrepancies in the estimation; however, this prediction still can significantly reduce many uncertainties and trial-and-errors, associated with choices of the run-out time and the number and range of applied stresses to be employed.

REFERENCES

- (1) Ritter, J. E., Bandyopadhyay, N., and Jakus, K., “Statistical Reproducibility of the Dynamic and Static Fatigue Experiments,” *Ceramic Bulletin*, Vol. 60, No. 8, 1981, pp. 798–806.
- (2) Ritter, J. E., “Engineering Design and Fatigue Failure of Brittle Materials,” *Fracture Mechanics of Ceramics*, Vol. 4, R. C. Bradt, D. P. H. Hasselmann, and F. F. Lange, editors, Plenum Press, New York, 1978, pp. 661–686.
- (3) Jakus, K., Coyne, D. C., and Ritter, J. E., “Analysis of Fatigue Data for Lifetime Prediction for Ceramic Materials,” *Journal of Materials Science*, Vol. 13, 1978, pp. 2071–2080.
- (4) Baratta, F. I., Quinn, G. D., and Matthews, W. T., “Errors Associated with Flexure Testing of Brittle Materials,” *U.S. Army MTL TR 87-35*, July 1987.
- (5) Quinn, G. D., Baratta, F. I., and Conway, J. A., “Commentary on U. S. Army Standard Test Method of Flexure Strength of High Performance Ceramics at Ambient Temperature,” *U. S. Army, AMMRC 85-21*, August 1985.
- (6) Ritter, J. E., Jakus, K., and Cooke, D. S., “Predicting Failures in Optical Glass Fibers,” *Proceedings of the 2nd International Conference on Environmental Degradation of Engineering Materials*, 1981, pp. 565–75.
- (7) Wiederhorn, S. M., “Influence of Water Vapor on Crack Propagation in Soda-Lime Glass,” *Journal of the American Ceramic Society*, Vol. 50, 1967, pp. 407–414.
- (8) Fuller, E. R. and Thomson, R. M., “Lattice Theories of Fracture,” *Fracture Mechanics of Ceramics*, Vol. 4, R. C. Bradt, D. P. H. Hasselmann, and F. F. Lange, editors, Plenum Press, New York, 1978, pp. 507–548.
- (9) Choi, S. R., Nemeth, N. N., and Gyekenyesi, J. P., “Slow Crack Growth of Brittle Materials with Exponential Crack Velocity Formulation – Part I: Analysis,” *NASA TM 2002-211153*, National Aeronautics & Space Administration, Glenn Research Center, Cleveland, OH (2002).
- (10) Sines, G., “Rationalized Crack Growth and Time-To-Fracture of Brittle Materials,” *Journal of the American Ceramic Society*, Vol. 59, No. 7-8, 1976, pp. C370–71.
- (11) Morrell, R., “Mechanical Properties of Engineering Ceramics: Test Bars Versus Components,” *Materials Science and Engineering*, Vol. A109, 1989, pp. 131–137.
- (12) Munz, D. and Fett, T., *Ceramics*, Springer-Verlag, Berlin, Germany, 1999, pp. 89–92.
- (13) Choi, S. R., Salem, J. A. and Nemeth, N. N., “High-Temperature Slow Crack Growth of a Silicon Carbide Determined by Constant-Stress-Rate and Constant-Stress Testing,” *Journal of Materials Science*, Vol. 33, 1998, pp. 1325–1332.
- (14) Zeng, K., Breder, K., and Rowcliffe, D. J., “Comparison of Slow Crack Growth Behavior in Alumina and SiC-Whisker-Reinforced Alumina,” *Journal of the American Ceramic Society*, Vol. 76, No. 7, 1993, pp. 1673–1680.
- (15) Breder, K., Mroz, T. J., Wereszczak, A. A., and Tennery, V. J., “Utilization of Fractography in the Evaluation of High-Temperature Dynamic Fatigue Experiments,” *Proceedings of Fractography of Glasses and Ceramics III, Ceramics Transactions*, Vol. 64, J. R. Varner, V. D. Frechette, and G. D. Quinn, editors, The American Ceramic Society, Westerville OH, 1996, pp. 353–366.
- (16) Choi, S. R., and Gyekenyesi, J. P., “Some Limitations in the Elevated-Temperature, Constant Stress-Rate Flexural Testing for Advanced Ceramics with Reference to the New, Ambient-Temperature Test Standard ASTM C1368,” *Ceramic Engineering & Science Proceedings*, Vol. 19, No. 3, 1998, pp. 595–605.
- (17) Fett, T., and Munz, D., “Determination of Crack Growth Parameter N in Ceramics under Creep Condition,” *Journal of Testing & Evaluation*, Vol. 13, No. 2, 1985, pp. 143–151.
- (18) Donaldson, K. Y., Venkateswaren, A., and Hasselman, D. P. H., “Role of Strain-Softening by Crack Formation in the Nonlinear Stress-Strain Behavior of a Polycrystalline Alumina at High Temperature,” *Fractography of Glasses and Ceramics, Advances in Ceramics*, Vol. 22, J. R. Varner and V. D. Frechette, editors., The American Ceramic Society, Westerville, OH, 1988, pp. 159–175.
- (19) Wereszczak, A. A., Breder, K., and Ferber, M. K., “Role of Oxidation in the Time-Dependent Failure Behavior of Hot Isostatically Pressed Silicon Nitride at 1370°C,” *Journal of the American Ceramic Society*, Vol. 76, No. 11, 1993, pp. 2919–2922.
- (20) Michalske, T. A., Smith, W. L. and Bunker, B. C., “Fatigue Mechanisms in High-Strength Silica-Glass Fibers,” *Journal of the American Ceramic Society*, Vol. 74, No. 8, 1991, pp. 1993–96.

- (21) Grathwohl, G. and Thümmel, F., "Creep of Reaction-Bonded Silicon Nitride," *Journal of Materials Science*, June 1978, Vol. 13, No. 6, pp. 1177–1186.
- (22) Fetta, T., Ernsta, E., Munza, D., Badenheimer, D., and Oberacker, R., "Weibull Analysis of Ceramics under High Stress Gradients," *Journal of the European Ceramic Society*, Vol. 23, No. 12, November 2003, pp. 2031–2037.
- (23) Quinn, G. D., "Review of Static Fatigue in Silicon Nitride and Silicon Carbide," *Ceramic Engineering and Science Proceedings*, Vol. 3, No. 1-2, 1982, pp. 77–98.
- (24) Quinn, G. D., and J. B. Quinn, "Slow Crack Growth in Hot-Pressed Silicon Nitride," *Fracture Mechanics of Ceramics*, Vol. 6, 1983, pp. 603–636.
- (25) Carroll, D. F., and Wiederhorn, S. M., "High Temperature Creep Testing of Ceramics," *International Journal of High Technology Ceramics* Vol. 4, No. 2, 1988, pp. 227–241.
- (26) Quinn, G. D., "Fracture Mechanism Maps for Advanced Structural Ceramics," *Journal of Materials Science*, Vol. 25, No. 10, 1990, pp. 4361–4376.
- (27) Quinn, G. D., "Fracture Mechanism Map for Hot-Pressed Silicon Nitride," *Ceramic Engineering and Science Proceedings*, Vol. 5, No. 7/8, 1984, pp. 596–602.
- (28) Quinn, G. D., and Quinn, J. B., "Slow Crack Growth in Hot-Pressed Silicon Nitride," *Fracture Mechanics of Ceramics*, Vol. 6, R. C. Bradt, A. G. Evans, D. P. H. Hasselman, and F. F. Lange, editors, Plenum Publishing Corp., NY, 1983, pp. 603–636.
- (29) Choi, S. R., Nemeth, N. N., and Gyekenyesi, J. P., "Slow Crack Growth of Brittle Materials With Exponential Crack-Velocity Formulation—Static Fatigue," *Journal of Materials Science*, Vol. 40, 2005, pp. 1647–1654.
- (30) Nelson, W., "Fitting of Fatigue Curves with Nonconstant Standard Deviation to Data with Runouts," *Journal of Testing and Evaluation*, Vol. 12, No. 2, March 1984, pp. 69–77.
- (31) Nelson, W., *Applied Life Data Analysis*, John Wiley & Sons, New York, 1982.
- (32) Statistica, Software for Statistical Data Analysis, Statsoft, Tulsa, OK.
- (33) Fuller, E. R., Lawn, B. R., and Cook, R. F., "Theory of Fatigue for Brittle Flaws Originating from Residual Stress Concentrations," *Journal of the American Ceramic Society*, Vol. 66, No. 5, 1983, pp. 314–321.
- (34) Breder, K. and Wereszczak, A. A., "Fatigue and Slow Crack Growth" in *Mechanical Testing Methodology for Ceramic Design and Reliability*, D. C. Cranmer and D. W. Richerson, editors, Marcel Dekker, Inc., New York, 1998, Chapter 6.
- (35) Quinn, G. D., and Morrell, R., "Design Data for Engineering Ceramics: A Review of the Flexure Test," *Journal of the American Ceramic Society*, Vol. 74, No. 9, 1991, pp. 2037–2066.
- (36) Jadaan, O. M., "Life Prediction for Ceramic Tubular Components," *Life Prediction Methodologies and Data for Ceramic Materials*, ASTM STP 1201, C. R. Brinkman and S. D. Duffy, editors, American Society for Testing and Materials, Philadelphia, PA, 1994, pp. 309–332.
- (37) Choi, S. R. and Salem, J. A., "Ultra-Fast Fracture Strength of Advanced Ceramics at Elevated Temperatures," *Materials Science & Engineering*, Vol. A242, 1998, pp. 129–136.
- (38) Salem, J. A. and Jenkins, M. G., "The Effect of Stress Rate on Slow Crack Growth Parameters," *Fracture Resistance Testing of Monolithic and Composite Brittle Materials*, ASTM STP 1409, J. A. Salem, G. D. Quinn, and M. G. Jenkins, editors, American Society for Testing and Materials, West Conshohocken, Pennsylvania, January 2002, pp. 213–227.
- (39) Zhang Y. H., Edwards, L., and Plumbridge, W. J., "Crack Healing in a Silicon Nitride Ceramic," *Journal of the American Ceramic Society*, Vol. 81, No. 7, 1998, pp. 1861–68.
- (40) Ando, K., Furusawa, K., Chu, M. C., Hanagata, T., Tuji, K., and Sato, S., "Crack-Healing Behavior Under Stress of Mullite/Silicon Carbide Ceramics and the Resultant Fatigue Strength," *Journal of the American Ceramic Society*, Vol. 84, No. 9, 2001, pp. 2073–78.
- (41) Choi, S. R. and Gyekenyesi, J. P., "Limitation on the Determination of Life Prediction Parameters of a Silicon Carbide with High Resistance to Slow Crack Growth," *Journal of Materials Science Letters*, Vol. 8, 1999, pp. 767–769.
- (42) Quinn, G. D., "Twisting and Friction Errors in Flexure Testing," *Ceramic Engineering And Science Proceedings*, Vol. 13, No. 7-8, 1992, pp. 319–330.
- (43) Wiederhorn, S. M., "Subcritical Crack Growth in Ceramics," *Fracture Mechanics of Ceramics*, Vol. 2, R. C. Bradt, D. P. H. Hasselman, and F. F. Lange, editors, Plenum Press, New York, 1974, pp. 613–646.
- (44) Zeng, K. and Rowcliffe, D. J., "Comparison of Hypothetical Slow Crack Growth Behavior of Two Materials," TRITA-MAC No. Department of Materials Science and Engineering, Royal Institute of Technology, Stockholm, Sweden, 1995.
- (45) Newman, J. C. and Raju, I. S., "An Empirical Stress-Intensity Factor Equation for the Surface Crack," *Engineering Fracture Mechanics*, Vol. 15, No. 1-2, 1981, pp. 185–92.
- (46) Wiederhorn, S. M. and Ritter, J. E. Jr., "Application of Fracture Mechanics Concepts to Structural Ceramics," *Fracture Mechanics Applied to Brittle Materials*, ASTM STP 678, S. W. Freiman, editor., American Society for Testing and Materials, Philadelphia PA, 1979, pp. 202–214.
- (47) Freiman, S. W., "A Critical Evaluation of Fracture Mechanics Techniques for Brittle Materials," *Fracture Mechanics of Ceramics*, Vol. 6, R. C. Bradt, A. G. Evans, D. P. H. Hasselman, and F. F. Lange, editors, Plenum Press, N.Y. 1983, pp. 27–45.
- (48) Pletka, B. J. and Wiederhorn, S. M., "A Comparison of Failure Predictions by Strength and Fracture Mechanics Techniques," *Journal of Materials Science*, Vol. 17, No. 5, 1982, pp. 1247–1268.
- (49) White, G. S., "Environmental Effects on Crack Growth in Ceramics," *Mechanical Testing Methodology for Ceramic Design and Reliability*, D. C. Cranmer and D. W. Richerson, editors, Marcel Dekker, Inc., New York, 1998, Chapter 3.
- (50) Wiederhorn, S. M. and Bolz, L. H., "Stress Corrosion and Static Fatigue of Glass," *Journal of the American Ceramic Society*, Vol. 53, No. 10, 1970, pp. 543–48.
- (51) Gupta, P. K., Inniss, D., Kurkjian, C. R. and Brownlow, D. L., "Determination of Crack Velocity as a Function of Stress Intensity from Static Fatigue Data," *Journal of the American Ceramic Society*, Vol. 77, No. 9, 1994, pp. 2445–49.

ASTM International takes no position respecting the validity of any patent rights asserted in connection with any item mentioned in this standard. Users of this standard are expressly advised that determination of the validity of any such patent rights, and the risk of infringement of such rights, are entirely their own responsibility.

This standard is subject to revision at any time by the responsible technical committee and must be reviewed every five years and if not revised, either reapproved or withdrawn. Your comments are invited either for revision of this standard or for additional standards and should be addressed to ASTM International Headquarters. Your comments will receive careful consideration at a meeting of the responsible technical committee, which you may attend. If you feel that your comments have not received a fair hearing you should make your views known to the ASTM Committee on Standards, at the address shown below.

This standard is copyrighted by ASTM International, 100 Barr Harbor Drive, PO Box C700, West Conshohocken, PA 19428-2959, United States. Individual reprints (single or multiple copies) of this standard may be obtained by contacting ASTM at the above address or at 610-832-9585 (phone), 610-832-9555 (fax), or service@astm.org (e-mail); or through the ASTM website (www.astm.org). Permission rights to photocopy the standard may also be secured from the Copyright Clearance Center, 222 Rosewood Drive, Danvers, MA 01923, Tel: (978) 646-2600; <http://www.copyright.com/>